drones

MDPI

Article

Coordinated Vision-Based Tracking by Multiple Unmanned Vehicles

Venanzio Cichella [1,*] and Isaac Kaminer [2]

[1] Department of Mechanical Engineering, University of Iowa, Iowa City, IA 52242, USA
[2] Department of Mechanical and Aerospace Engineering, Naval Postgraduate School, Monterey, CA 93940, USA
* Correspondence: venanzio-cichella@uiowa.edu

Abstract: We address the problem of coordinated vision-based tracking of a moving target using multiple unmanned vehicles that exchange information over a supporting time-varying network. The objective of this work is to formulate decentralized control algorithms that enable multiple vehicles to follow the target while coordinating their phase separation. A typical scenario involves multiple unmanned aerial vehicles that are required to monitor a moving ground object (target tracking) while maintaining a desired inter-vehicle separation (coordination). To solve the vision-based tracking problem, the yaw rate of each vehicle is used as the control input, while the speeds of the vehicles are adjusted to achieve coordination. It is assumed that the vehicles are equipped with an internal autopilot, which is able to track yaw rate and speed commands. The performance of the coordinated vision-based tracking algorithm is evaluated as a function of the target's velocity, tracking performance of the onboard autopilot, and the quality of service of the communication network.

Keywords: vision-based tracking; coordination; multiple vehicles

check for updates

Citation: Cichella, V.; Kaminer, I. Coordinated Vision-Based Tracking by Multiple Unmanned Vehicles. *Drones* **2023**, *7*, 177. https://doi.org/10.3390/drones7030177

Academic Editor: Andrey V. Savkin

Received: 16 January 2023
Revised: 27 February 2023
Accepted: 3 March 2023
Published: 5 March 2023

Copyright: © 2023 by the authors. Licensee MDPI, Basel, Switzerland. This article is an open access article distributed under the terms and conditions of the Creative Commons Attribution (CC BY) license (https://creativecommons.org/licenses/by/4.0/).

1. Introduction

Unmanned Vehicles (UxVs)—including air, ground, and marine robots—play a crucial role today in many complex missions, especially in hazardous situations, where the presence of human operators must be avoided. Numerous problems related to motion control of autonomous vehicles have been studied in recent years. One focus area of research delineated in the literature is the vision-based motion control UxVs. A variety of approaches based on visual feedback have been proposed in [1–13]. Typical applications considered in the literature include autonomous landing [10], aerial refueling [11], and vision-based target tracking (VBT) [7], where the objective is to control the motion of the UxVs relative to a static or moving target.

In spite of relevant theoretical and technological advances, the problem of vision-based motion control is still very challenging. In fact, the control system has to deal with poor, and insufficient, accuracy of the acquired data. Moreover, in the situation where only passive sensor data are available about the target, the control task must be defined using the information obtained in the camera frame only. Finally, the control engineer must take into account that processing image or video in general requires high computational resources, and that the information on the target's and vehicle's position and velocity might be unreliable or not available at all.

Another challenge to be addressed is the problem of vision-based motion control of multiple cooperative UxVs. Relevant work in the area of cooperative control of autonomous systems includes [14–20] (and the references therein). In these cases, one needs to establish communication between the vehicles. This compels the control designer to take into consideration the fact that the amount of information that can be exchanged could be limited and may vary over time. Cooperative motion control strategies must be developed

that yield robust performance even in the presence of temporary loss of communication links and switching communication topologies.

Motivated by these challenges, we describe a solution to the Coordinated Vision-Based Tracking (CVBT) problem. The objective of this work is to enable a set of n vehicles, with dynamics described by the kinematic car model (i.e., Dubins' car), to orbit around (track and monitor) a target while coordinating their phase separation with each other. Figure 1 depicts the control framework adopted in this paper. The work focuses on two main parts. First, we derive a control algorithm for the yaw rate to enable the vehicles involved in the mission to track a (static or moving) target and orbit around it (VBT). Second, we formulate control laws for the speed of each vehicle so that they maintain a predefined space separation while orbiting around the target (coordination).

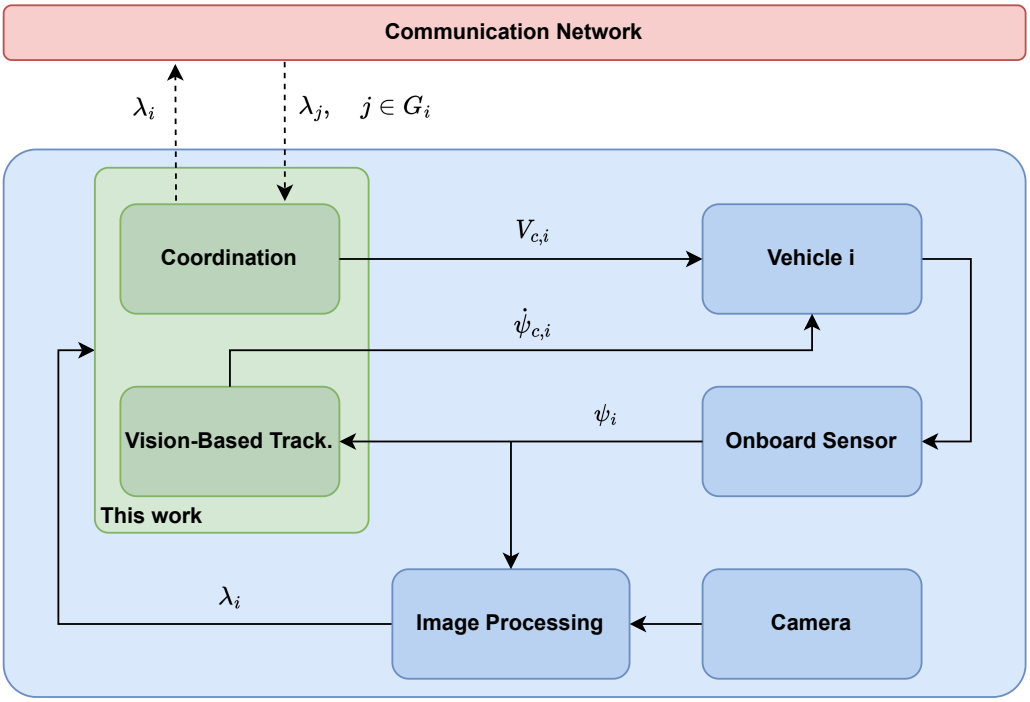


Figure 1. Coordinated vision-based target tracking—general framework.

At the VBT level, we show that VBT is achieved by using only vehicle-to-target relative line-of-sight (LOS) angles, which can be obtained from the visual measurement. This reduces the computational load required to acquire more complex information, such as the target's position and velocity. The solution to the VBT problem presented in this paper builds on previous papers [21,22], where the authors demonstrate that the proposed control algorithm guarantees exponential convergence and ultimate boundedness of the VBT error in the case of static and moving targets. One fundamental assumption made in [21] is that the velocity of the unmanned vehicle is constant. In [22], such an assumption is relaxed and convergence of the VBT error to zero is guaranteed as long as the speed of the vehicle is lower and upper bounded by some constants. However, the work in [22] assumes that the UxV is equipped with an ideal inner-loop autopilot (AP), which guarantees that the difference between commanded and actual angular rates is always identical to zero. In the present paper, we address a more realistic case, where the AP can only ensure that such a difference is bounded. It is shown that the VBT algorithm is robust to non-perfect tracking of the VBT input commands. Performance of the outer-loop VBT controller is derived as a function of the performance of the inner-loop AP.

At the coordination level, motivated by [14], where the authors propose a solution to the cooperative path-following problem, we propose a control law for the speeds of the UxVs and show that coordination can be achieved by allowing the vehicles to exchange

minimum information (the LOS angle only) between each other over a communication network. Performance of the coordination algorithm is analyzed, while taking into account non-ideal communication scenarios (such as failures, drop-outs, and switching topology). We further extend the coordination result by considering non-perfect tracking of the speed commands. We show that the controller's performance is guaranteed as long as the difference between the commanded and actual speed of the vehicles remains bounded.

The main features of this paper are as follows: (i) VBT is achieved by using only a UxV-target-relative (LOS) angle; (ii) performance of the overall control architecture is guaranteed against communication failures among the UxVs and non-ideal tracking of the reference control commands by the autopilot.

The paper is organized as follows: Section 2 formulates the CVBT problem; it describes the kinematics of the systems of interest and introduces a set of assumptions and limitations on the onboard autopilot, as well as on the supporting communication network. Section 3 presents a control algorithm that solves the problem at hand. Section 4 illustrates the simulation results. Finally, conclusions are summarized in Section 5. Theoretical proofs of the results are reported in the Appendixes A–E.

2. Problem Formulation

In what follows, we first consider a single UxV and characterize the dynamics of the kinematic errors, describing the VBT approach that was previously presented in [21]. Second, following a decentralized coordination strategy similar to the one presented in [23], we consider the case of multiple UxVs by introducing a set of appropriate coordination variables, along with assumptions and limitations on a given communication network. Table 1 lists the symbols and their definitions for clarity.

Table 1. Symbols and definitions.

Symbol	Definition
UxV	Unmanned (ground, aerial, underwater, surface) vehicle
$\mathcal{I}$	Inertial frame
$V_g(t)$, $\vec{v}_g(t)$	Speed and velocity of the UxV at time t
$V_{c,i}(t)$, $\dot{\psi}_{c,i}(t)$	Speed and angular rate commands for UxV i at time t
$\psi(t)$	Heading angle of the UxV at time t
$V_t(t)$, $\psi_t(t)$	Speed and heading angle of the UxV at time t
$\rho(t)$	Horizontal distance between UxV and target at time t
$\lambda(t)$	Line of sight phase angle at time t
$\hat{\eta}(t)$	Vision-based angle tracking error at time t
ρ_d	Desired range
$\rho_e(t)$	Vision-based distance tracking error at time t
$x(t)$	Vision-based tracking error vector at time t
$G_i(t)$	Neighborhood of vehicle i at time t
$\Lambda(t)$	Communication graph
$L(t)$	Laplacian of the graph at time t
T, μ	Parameters representing the quality of the communication network
$\zeta(t)$	Coordination error vector at time t
$h_{ij}(t)$	Heterogeneity parameter between nodes i and j at time t

2.1. Vision-Based Tracking

Consider the horizontal projection of the UxV and target-relative kinematics in the inertial frame $\mathcal{I}$ illustrated in Figure 2. Let $\vec{v}_g(t) \in \mathbb{R}^3$ and $\psi(t) \in \mathbb{R}$ be the UxV's velocity vector and heading angle, respectively. Let $V_g(t) \in \mathbb{R}$ be the magnitude of $\vec{v}_g(t)$. Let $V_t(t)$ be the speed of the target and $\psi_t(t)$ be its heading angle. Let $\rho(t) \in \mathbb{R}$ be the horizontal distance between the UxV and the target. Let $\lambda(t) \in \mathbb{R}$ be the LOS phase angle, let $\vec{\lambda}_g(t) \in \mathbb{R}^3$ denote the LOS vector, and let $\vec{\lambda}_p(t) \in \mathbb{R}^3$ be the vector perpendicular to $\vec{\lambda}_g(t)$. Finally, let $\eta(t) \in \mathbb{R}$ denote the angle between $\vec{\lambda}_p(t)$ and $\vec{v}_g(t)$, which can be written as

$$\eta(t) = \psi(t) - (\lambda(t) - \frac{\pi}{2}). \tag{1}$$

Since the rotational speed of the LOS can be expressed as

$$\dot{\lambda}(t) = \frac{V_g(t)\cos(\eta(t))}{\rho(t)} - \frac{V_t(t)\cos(\psi_t(t) - (\psi(t) - \eta(t)))}{\rho(t)}, \tag{2}$$

one can compute the derivative of Equation (1):

$$\dot{\eta}(t) = -\frac{V_g(t)\cos\eta(t) - V_t(t)\cos(\psi_t(t) - \psi(t) + \eta(t))}{\rho(t)} + \dot{\psi}(t).$$

Next, define $\hat{\eta}(t) \triangleq \eta(t)/\rho_d$.

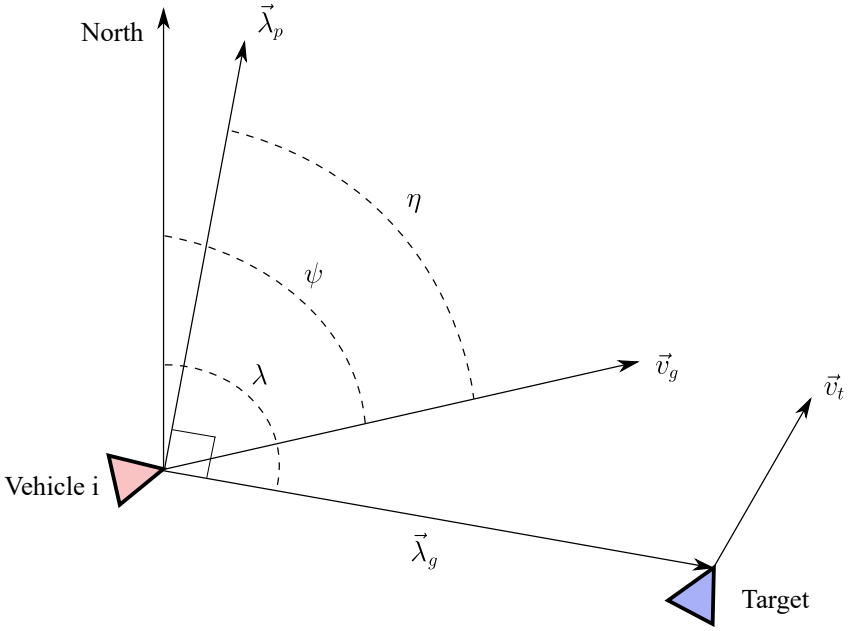


Figure 2. Vision-based target tracking—problem formulation.

In what follows, $\hat{\eta}(t)$ plays the role of guidance tracking error. Obviously, if $\hat{\eta}(t) = 0$, then $\eta(t) = 0$, and it follows from Equation (1) that the angle between the UxV velocity vector and the LOS vector equals $\frac{\pi}{2}$ rad. This results in the UxV orbiting around the target, which constitutes part of the control objective. In fact, to accomplish VBT, the control law must also enable the UxV to orbit along a desired circle. This can be achieved when driving the horizontal range $\rho(t)$ to a desired constant value, $\rho_d \in [\rho_{dmin}, \rho_{dmax}] \subset \mathbb{R}$. By projecting the horizontal components of the UxV velocity vector onto the LOS, one can express the dynamics of $\rho(t)$ as follows:

$$\dot{\rho}(t) = -V_g(t)\sin\eta(t) + V_t(t)\sin(\psi_t(t) - \psi(t) + \eta(t)).$$

Finally, by defining $\rho_e(t) \triangleq 1/\rho(t) - 1/\rho_d$, we can write the dynamics of the VBT error states

$$\begin{cases} \dot{\hat{\eta}}(t) = -\dfrac{V_g(t)\cos(\hat{\eta}(t)\rho_d)}{\rho_d}\left(\rho_e(t) + \dfrac{1}{\rho_d}\right) + \dfrac{\dot{\psi}(t)}{\rho_d} \\ \qquad\qquad + \dfrac{V_t(t)\cos(\hat{\eta}(t)\rho_d - \psi_r(t))\left(\rho_e(t) + \frac{1}{\rho_d}\right)}{\rho_d} \\ \dot{\rho}_e(t) = \left(\rho_e(t) + \dfrac{1}{\rho_d}\right)^2 V_g(t)\sin(\eta(t)) \\ \qquad\qquad - \left(\rho_e(t) + \dfrac{1}{\rho_d}\right)^2 V_t(t)\sin(\hat{\eta}(t)\rho_d - \psi_r(t))\,, \end{cases} \tag{3}$$

where $\psi_r(t) \triangleq \psi(t) - \psi_t(t)$. Before providing a formal statement of the problem at hand, we give a set of assumptions that must be satisfied:

Assumption 1. *The speed of the UxV is bounded as follows:*

$$0 < V_{g,min} \leq V_g(t) \leq V_{g,max}\,.$$

Assumption 2. *The speed of the target to be tracked satisfies*

$$0 \leq V_{t,min} \leq V_t(t) \leq V_{t,max}\,.$$

Assumption 3. *The UxV is equipped with an autopilot capable of following speed and yaw rate commands, $V_c(t)$ and $\dot{\psi}_c(t)$. The tracking performance of the autopilot satisfies*

$$|V_c(t) - V_g(t)| < \delta_V\,, \quad |\dot{\psi}_c(t) - \dot{\psi}(t)| < \delta_\psi\,,$$

for all $t \geq 0$ and for some δ_V , $\delta_\psi > 0$.

Finally, the VBT control problem can be defined as follows:

Problem 1. ***Vision-Based Tracking (VBT):*** *Consider a UxV and a target with speeds satisfying Assumptions 1 and 2. Assume that the UxV is equipped with an autopilot satisfying Assumption 3. Then, the objective of VBT is to define a control law for the commanded angular velocity of the UxV, $\dot{\psi}_c(t)$, such that the error vector $x(t) \triangleq [\hat{\eta}(t), \rho_e(t)]^\top$, with dynamics in Equation (3), converges to a neighborhood of zero.*

Remark 1. *The control algorithm utilizes feedback from image processing software (centroid position in camera frame) and an on-board inertial measurement unit, typical for modern autopilots. Hence, only the line of sight (LOS) to the target is assumed to be known, justifying the use of the term "vision-based tracking". The crucial aspect of the approach is achieving convergence of the horizontal range to a desired value ρ_d, without knowledge of the actual range $\rho(t)$, target position, or velocity.*

2.2. Coordination

Consider now a set of n UxVs and let $V_{g,i}(t)$, $\psi_i(t)$, and $\lambda_i(t)$ be the speed, the heading angle, and the LOS angle of the i-th vehicle ($i \in \{1, \ldots, n\}$), respectively. Furthermore, let $\hat{\eta}_i(t)$ and $\rho_{e,i}(t)$ be its VBT errors with the dynamics described in Equation (3). The objective of coordination is to drive the difference between the UxVs LOS phase angles to a desired value, in order to maintain a desired phase separation. Thus, we consider the i-th and j-th vehicles to be coordinating at time t if their LOS angles satisfy the condition

$$\lambda_i(t) - \lambda_j(t) = \lambda_d,$$

where $\lambda_d \in \mathbb{R}$ is the desired separation in terms of LOS angle. Finally, without loss of generality, it is convenient to set $\lambda_d = 0$; when a specific phase shift is desired, λ_d can be assigned a desired constant value. Therefore, the coordination problem for multiple UxVs reduces to achieving $\lambda_i(t) - \lambda_j(t) = 0\,, \forall i, j \in \{1\,, \ldots\,, n\}\,, \quad i \neq j\,, \quad \forall t > 0$.

To guarantee coordination, the states $\lambda_1(t)\,, \ldots\,, \lambda_n(t)$ have to be exchanged between the UxVs over a communication network. In this paper, we use the notation and tools from algebraic graph theory. Introduction to the material and further relevant reading can be found in [24]. Let $L(t)$ be the Laplacian matrix of the communication graph $\Gamma(t)$. Let $Q \in \mathbb{R}^{(n-1)\times n}$ be such that $Q1_n = 0$ and $QQ^\top = I_{n-1}$, with $1_n = [1\,, 1\,, \ldots\,, 1] \in \mathbb{R}^n$. Let $G_i(t)$ denote the set of vehicles positioned in a neighborhood of the i-th UxV. Now, we can define a set of assumptions that the communication network must satisfy [25]:

Assumption 4. *The i-th UxV can only communicate with the neighboring set $G_i(t)$.*

Assumption 5. *The communication between two vehicles is bidirectional, with no time delays.*

Assumption 6. *The connectivity of the communication graph $\Gamma(t)$ satisfies*

$$\frac{1}{n}\frac{1}{T}\int_t^{t+T} \bar{L}(\tau)d\tau \geq \mu I_{n-1} \quad \forall t \geq 0\,,$$

where $\bar{L}(t) \triangleq QL(t)Q^\top$ has the same spectrum of $L(t)$ without the eigenvalue $\lambda_1(L(t)) = 0$, and the parameters $T > 0\,$, $\mu \in (0, 1]$ describe the quality of service of the communication network.

It is worth noting that Assumption 6 stipulates that the communication graph $\Gamma(t)$ is only required to be connected in an integral sense over the time range T rather than pointwise in time. In fact, the graph may be disconnected during some interval of time or may even fail to be connected at all times. In this sense, it is general enough to capture packet dropouts, loss of communication, switching topologies, etc. Small values of T and large values of μ indicate better quality of the communication network.

Finally, the coordination problem can be defined as follows:

Problem 2. ***Coordination:*** *Consider a set of* n *UxVs with speed satisfying Assumption 1 and a target with speed satisfying Assumption 2. Assume that the vehicles are equipped with an autopilot satisfying Assumption 3. Finally, suppose that the UxVs are supported by a communication network satisfying Assumptions 4–6. Then, the objective is to design feedback control laws for the commanded speeds $V_{c,i}(t)\,, \forall i \in \{1\,, \ldots\,, n\}$ such that the difference between the LOS angles of the n UxVs converge to a neighborhood of zero, i.e.,*

$$\lambda_i(t) - \lambda_j(t) \to 0\,, \quad \forall i, j \in \{1\,, \ldots\,, n\}\,, i \neq j\,, \forall t > 0\,,$$

and such that the speeds of the vehicles converge to predefined constant values, i.e.,

$$V_{g,i}(t) \to V_{d,i}\,, \quad \forall i \in \{1\,, \ldots\,, n\}\,, \forall t > 0\,.$$

3. Main Result

In this section, we first present the outer-loop nonlinear controller that uses the angular velocity $\dot{\psi}_{c,i}(t)$ to solve Problem 1. Then, we formulate a control law for the speed commands $V_{c,i}(t)\,, \forall i \in \{1\,, \ldots\,, n\}$, which solves Problem 2.

3.1. Vision-Based Tracking

Recall from Section 2 that the main objective of the VBT control algorithm is to drive the states $(\hat{\eta}(t), \rho_e(t))$ to a neighborhood of zero. To this end, we propose the following guidance law [21]:

$$\dot{\psi}_c(t) = \frac{V_g(t)}{\rho_d}\cos(\eta(t)) - k_\eta \eta(t)\,. \tag{4}$$

Then, the solution to the VBT problem for a single UxV can be summarized in the following Lemma:

Lemma 1. ***Vision-Based Tracking (VBT):*** *Consider a UxV with speed $V_g(t)$ satisfying Assumption 1 and a moving target with speed satisfying Assumption 2. Let the commanded angular rate $\dot{\psi}_c(t)$ be governed by Equation (4) and assume that the vehicle is equipped with an autopilot satisfying Assumption 3. Moreover, assume that at time $t = 0$ the error vector satisfies*

$$x(0) = [\hat{\eta}(0), \rho_e(0)]^\top \in \Omega_v \triangleq \{x : x^\top P x \leq c^2\}, \tag{5}$$

with $c = \frac{c_\rho}{\rho_d}\sqrt{\lambda_{min}(P)}$; c_ρ satisfies

$$c_\rho \sqrt{\frac{c_\rho^2}{4} + (2 + c_\rho + c_\rho/6)^2} < \frac{\rho_d}{V_{g,max}} \frac{(\lambda_{min}(W) - 2\lambda_v \lambda_{max}(P))}{2\lambda_{max}(P)}, \tag{6}$$

with P and W being positive definite matrices, $0 < \lambda_v < \frac{\lambda_{min}(W)}{2\lambda_{max}(P)}$, and

$$k_\eta > max\left(\frac{2V_g/\rho_d}{\sqrt{4V_g/V_{g,min} - 1}}, 1\right).$$

Then, if the velocity of the target $V_t(t)$ and the angular speed tracking performance of the autopilot (i.e., δ_ψ) satisfy

$$\frac{V_{t,max}(1 + c_\rho)\sqrt{1 + (1 + c_\rho)^2}}{\lambda_v \rho_d^2} + \frac{\delta_\psi}{2\lambda_v \rho_d} < \frac{c_\rho}{\rho_d},$$

the VBT error $x(t)$, with the dynamics described in Equation (3), is ultimately bounded with bound $||x(t)|| \leq \frac{c_\rho}{\rho_d}$.

Corollary 1. *Under the assumptions stated in Lemma 1, if the velocity of the target is $V_t = 0, \quad \forall t \geq 0$ and the autopilot has ideal performance of (i.e., $\delta_\psi = \delta_V = 0$), the VBT error converges exponentially to zero as follows:*

$$||x(t)|| \leq \sqrt{\frac{\lambda_{max}(P)}{\lambda_{min}(P)}} ||x(0)|| e^{-\lambda_v t}. \tag{7}$$

Proof. The proofs of Lemma 1 and Corollary 1 are given in Appendixes A and B, respectively.

3.2. Coordinated Vision-Based Tracking

To drive the LOS angles of the UxVs to the same increasing value, the speed of the vehicles is adjusted based on the coordination information exchanged over the communication network. Since, by assumption, each UxV can only communicate with a neighboring set of vehicles, denoted as $G_i(t)$, we let the commanded velocity $V_{c,i}(t)$ for the i-th vehicle be governed by

$$V_{c,i}(t) = \frac{u_{\text{coord},i}(t)\rho_{d,i}}{\cos(\eta_i(t))}, \tag{8}$$

where

$$u_{\text{coord},1}(t) = -a \sum_{j \in G_1(t)} (\lambda_1(t) - \lambda_j(t)) + \frac{V_{d,1}}{\rho_{d,1}}, \tag{9a}$$

$$u_{\text{coord},i}(t) = -a \sum_{j \in G_i(t)} (\lambda_i(t) - \lambda_j(t)) + \chi_{I,i}(t), \quad i = 2, \ldots, n, \tag{9b}$$

$$\dot{\chi}_{I,i}(t) = -b \sum_{j \in G_i(t)} (\lambda_i(t) - \lambda_j(t)), \quad \chi_{I,i}(0) = \frac{V_{d,i}}{\rho_{d,i}}, \; i = 2, \ldots, n, \tag{9c}$$

with vehicle 1 elected as leader of the fleet, and $a, b > 0$. Note that $V_{d,1}$, $V_{d,2}$, ... , $V_{d,n}$ are constant desired speeds that satisfy $\frac{V_{d,1}}{\rho_{d,1}} = \frac{V_{d,2}}{\rho_{d,2}} = \ldots = \frac{V_{d,n}}{\rho_{d,n}}$, in order to maintain the same turn rate around the target. Moreover, the following inequalities must hold to guarantee feasibility of the mission:

$$0 < V_{g,min}/\delta < V_{d,min} \leq V_{d,j} \leq V_{d,max} < \delta V_{g,max} ,$$

$\forall j \in \{1 , \ldots , n\}$, where $0 < \delta < 1$.

Remark 2. *Parameter δ guarantees that a margin is left between the minimum (and maximum) UxV's velocity and the desired speed, therefore ensuring the existence of a solution for the coordination problem. In fact, assume that the desired speed for the i-th UxV is $V_{d,i} = V_{g,min}$. It follows that, if the vehicle is required to slow down in order to coordinate with the rest of the fleet, it would not be possible since no margin is left between the desired and minimum feasible velocities.*

Next, we define the coordination error vector as

$$\zeta(t) \triangleq [\zeta_1^\top(t) , \zeta_2^\top(t)]^\top , \tag{10}$$

where

$$\zeta_1(t) = Q\lambda(t) , \quad \zeta_2(t) = \chi_I(t) - \frac{V_d}{\rho_d} 1_n ,$$
$$\lambda(t) \triangleq [\lambda_1(t) , \ldots , \lambda_n(t)]^\top \in \mathbb{R}^n ,$$
$$\chi_I(t) \triangleq [\chi_{I,2}(t) , \ldots , \chi_{I,n}(t)]^\top \in \mathbb{R}^{n-1} ,$$

where $1_n = [1, 1, \ldots, 1]^\top \in \mathbb{R}^n$ and

$$\frac{V_d}{\rho_d} \triangleq \frac{V_{d,1}}{\rho_{d,1}} = \ldots = \frac{V_{d,n}}{\rho_{d,n}} .$$

Note that, from the properties of Q, if at time t we have $\zeta_1(t) = 0$, then $\lambda(t) \in \text{span}\{1_n\}$, which implies that $\lambda_i(t) = \lambda_j(t)$ for all $i, j \in \{1, \ldots, n\}$. Moreover, if at the same time $\zeta_2(t) = 0$, then the commanded speed of each vehicle is equal to its desired constant speed, which is

$$V_{c,i} = V_{d,i} , \quad \forall i \in \{1 , \ldots , n\} .$$

Before stating the main result of the paper, let us define $c_v, c_c > 0$ as $c_v \triangleq \frac{c_\rho}{\rho_{d,max}} \sqrt{\lambda_{min}(P)}$, and

$$c_c \triangleq \min\left(\frac{V_{g,max} - V_{d,max}/c_\eta}{2\kappa_1 \rho_{d,max}(an+1)} - \frac{\kappa_2}{\kappa_1} \frac{c_\rho}{\rho_{d,max}} , \frac{V_{d,min} - V_{g,min}}{2\kappa_1 \rho_{d,max}(an+1)} - \frac{\kappa_2}{\kappa_1} \frac{c_\rho}{\rho_{d,max}} \right) ,$$

where P is a positive definite matrix, c_ρ satisfies Equation (6), and

$$c_\rho < \min\left(\frac{1}{2kn((1+a)n+1+a)\rho_k^2} , \frac{V_{g,max} - V_{d,max}/c_\eta}{2\kappa_2(an+1)} , \frac{V_{d,min} - V_{g,min}}{2\kappa_2(an+1)} \right) ,$$

where $k > 2$; $0 < c_\eta \leq 1$; and some positive ρ_k, κ_1 and κ_2.

Finally, the main result is stated in the following Theorem:

Theorem 1. ***Coordinated Vision-Based Tracking (CVBT):*** *Consider a set of n UxVs and a target with speed satisfying Assumption 2. Let the commanded angular rate of the UxVs be governed by Equation (4), and let the commanded speed be governed by Equation (8). Assume that the UxVs are equipped with autopilots satisfying Assumption 3. Suppose that the UxVs*

communicate over a network satisfying Assumptions 4–6. If at time $t = 0$ the VBT error and the coordination error satisfy

$$x_i(0) \in \Omega_v \triangleq \{x_i : x_i^\top P x_i \leq c_v^2\}, \quad \forall i \in \{1, \ldots, n\}, \tag{11}$$

and

$$\zeta(0) \in \Omega_c \triangleq \{\zeta : ||\zeta|| \leq c_c\}, \tag{12}$$

respectively, then we have the following:
(i) The velocities of the UxVs satisfy Assumption 1;
(ii) The VBT error $x(t)$, with dynamics described in Equation (3), is ultimately bounded with bound

$$||x(t)|| \leq \frac{c_\rho}{\rho_d}, \tag{13}$$

if the velocity of the target $V_t(t)$ and the angular rate tracking performance of the autopilot (i.e., δ_ψ) satisfy

$$\frac{V_{t,max}(1+c_\rho)\sqrt{1+(1+c_\rho)^2}}{\lambda_v \rho_d^2} + \frac{\delta_\psi}{2\lambda_v \rho_d} < \frac{c_\rho}{\rho_d}; \tag{14}$$

(iii) The coordination error vector $\zeta(t)$ defined in Equation (10) satisfies the following bound:

$$||\zeta(t)|| \leq \kappa_1^* ||\zeta(0)|| e^{-\lambda_c(1-\theta)t} + \kappa_2^* \sup_{\tau \in [0,t]} ||u_{xv}(\tau)||, \tag{15}$$

where $u_{xv}(t) = 3\max\left(\frac{V_{d,max}}{\rho_{d,min}}\rho_{d,max}||x||, \frac{V_{t,max}}{\rho_{min}}, \frac{\delta_V}{\rho_{min}}\right)$, and κ_1, κ_2 are positive constants.

Corollary 2. *Under the same assumptions stated in Theorem 1, if the velocity of the target is $V_t = 0, \quad \forall t \geq 0$, and the autopilot has ideal performance (i.e., $\delta_\psi = \delta_V = 0$), we have the following:*
(i) The velocities of the UxVs satisfy Assumption 1;
(ii) The VBT error $x(t)$, with dynamics described in Equation (3), converges exponentially to zero (see Equation (7));
(iii) The coordination error vector $\zeta(t)$ defined in Equation (10) converges exponentially to zero as follows:

$$||\zeta(t)|| \leq \bar{\kappa}_1 ||\zeta(0)|| e^{-\lambda_c t} + \bar{\kappa}_2 ||x(0)|| e^{-\frac{\lambda_v + \lambda_c}{2} t},$$

where $\bar{\kappa}_1$, $\bar{\kappa}_2$ are positive constants, with rate of convergence $\lambda_c = \frac{\bar{\gamma}}{(1+kn)\rho_k}$, with $\bar{\gamma} \geq \frac{an\mu}{T(1+anT)^2}$, and

$$\rho_k \geq \max\left(\frac{2k\bar{\gamma}}{1+kn}, 1, \left(1 + \frac{1}{4}\bar{\gamma}^2 + \frac{(kn+1)^2}{\bar{\gamma}^2 k^2 n^3}\right)\right), \quad k > 2. \tag{16}$$

Proof. The proofs of Theorem 1 and Corollary 2 are given in Appendixes C and D, respectively.

Remark 3. *The maximum guaranteed rate of convergence can be obtained by letting $a = \frac{1}{nT}$, which is*

$$\max_{a>0} \lambda_c = \frac{\mu}{4T^2(1+kn)\rho_k}.$$

Moreover, it is worth noticing that if one modifies the control laws given in Equation (9) as follows:

$$u_{coord,i}(t) = -a \sum_{j \in G_1(t)} (\lambda_i(t) - \lambda_j(t)) + \frac{V_{d,i}}{\rho_{d,i}}, \tag{17a}$$

$$\dot{\chi}_{I,i}(t) = -b \sum_{j \in G_i(t)} (\lambda_i(t) - \lambda_j(t)) \, \chi_{I,i}(0) = \frac{V_{d,i}}{\rho_{d,i}} \, i = 1, \ldots, n, \tag{17b}$$

i.e., all the UxVs involved in the mission are leaders; then, one can show [23] that the rate of convergence reduces to

$$\lambda_c = \frac{\mu}{4T^2(1+k)\rho_k}\,.$$

This implies that the rate of convergence depends on the quality of the communication network, and it scales with the number of vehicles.

4. Simulation Results

This section presents the simulation results. In the proposed scenario, six UxVs are asked to rotate around a target along two orbits of different radius, while maintaining a phase separation of $\frac{\pi}{3}$rad from each other. In particular, UxV1—elected as the leader—UxV3, and UxV5 are required to rotate on an orbit of radius 100 m, while UxV2, UxV4, and UxV6 rotate on an orbit of radius 150 m. The desired speeds at which the UxVs are asked to converge are $V_{d,1} = V_{d,3} = V_{d,5} = 25$ m/s and $V_{d,2} = V_{d,4} = V_{d,6} = 37.5$ m/s.

We assume that the vehicles can only communicate with each other when the distance between them is less than 250 m. All-to-all communication is never achieved throughout the mission. In Figure 3, the black lines connecting vehicle i and vehicle j indicate that the two UxVs are communicating. For clarity of presentation, these lines are shown only at four different time instances ($t = 0$ s, 180 s, 300 s, 600 s).

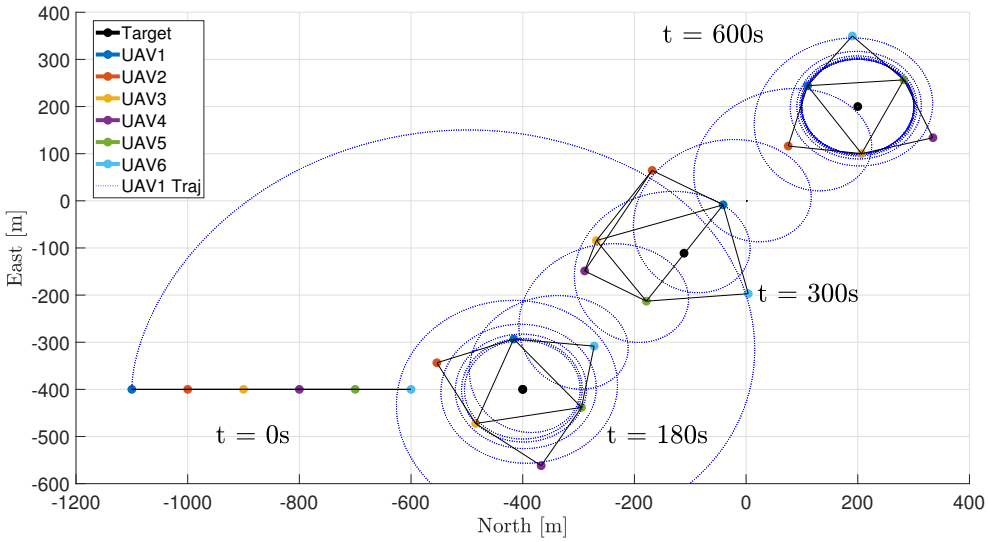


Figure 3. Coordinated vision-based tracking mission—2D paths.

To illustrate the performance of the CVBT controller in the presence of non-ideal tracking of reference commands, we implemented a proportional controller as follows

$$\dot{V}_g(t) = k_V(V_c(t-t_d) - V_g(t))\,,$$
$$\ddot{\psi}(t) = k_\psi(\dot{\psi}_c(t-t_d) - \dot{\psi}(t))\,,$$

with gains $k_V = 0.2$, $k_\psi = 0.05$, and time delay $t_d = 0.1$ s. The time delay is intentionally introduced to simulate the effects of real-world delays that can impact the performance of an unmanned vehicle's autopilot system.

The control gains of the CVBT controller have been chosen as follows: $k_\eta = 2$, $a = 0.1$, $b = 0.05$. The imposed speed limits are $V_{g,min} = 17$ m/s and $V_{g,max} = 32$ m/s.

Mission

At $t = 0$ s, the target is positioned at $[-400; -400]$ m with velocity $V_t(t) = 0$, and the UxVs are positioned in a straight-line formation near the target, as depicted in Figure 3. When the mission begins, the UxVs start approaching the desired orbits with different speed profiles. Figures 4 and 5 show the convergence to a neighborhood of zero of the VBT error. Figures 6 and 7 illustrate the coordination error and the actual speeds. The slow rate of convergence depends on the facts that the UxVs start the mission far away from each other and each vehicle is able to communicate with only few of its neighbors (see Figure 3, black lines).

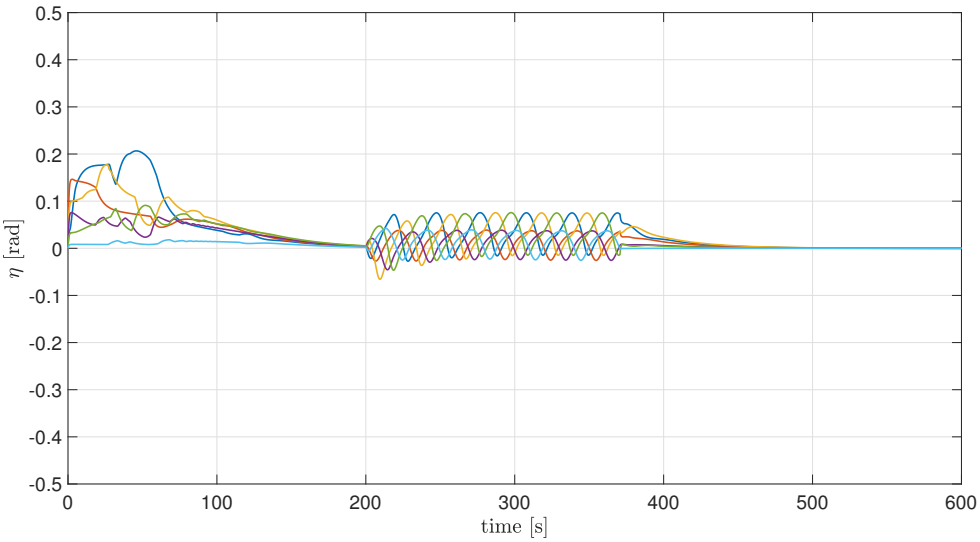


Figure 4. Vision-based tracking error for each vehicle.

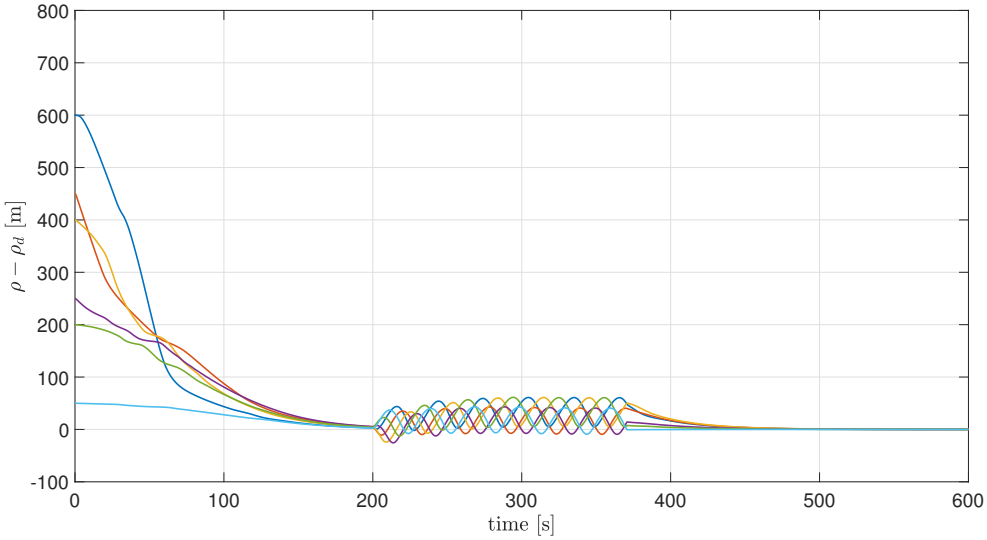


Figure 5. Vision-based tracking error for each vehicle.

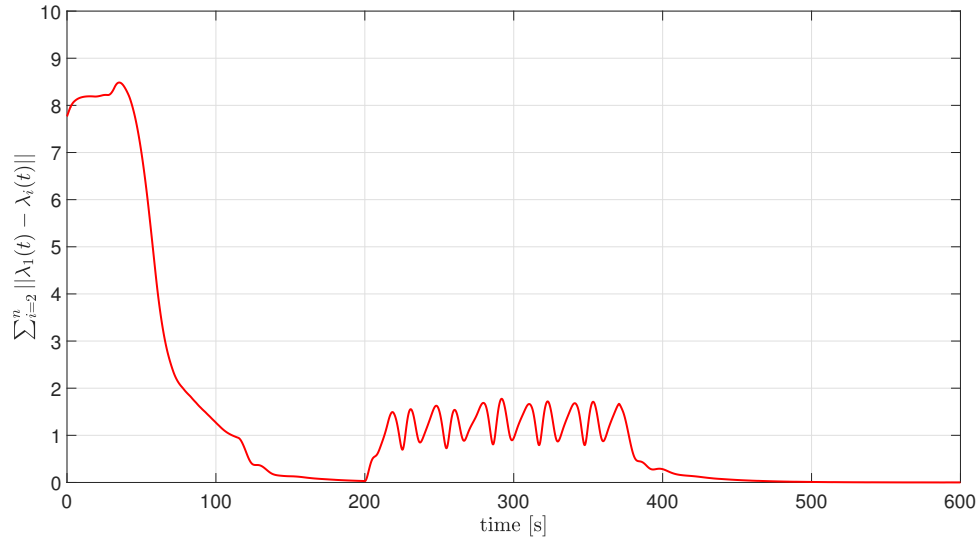


Figure 6. Coordination error.

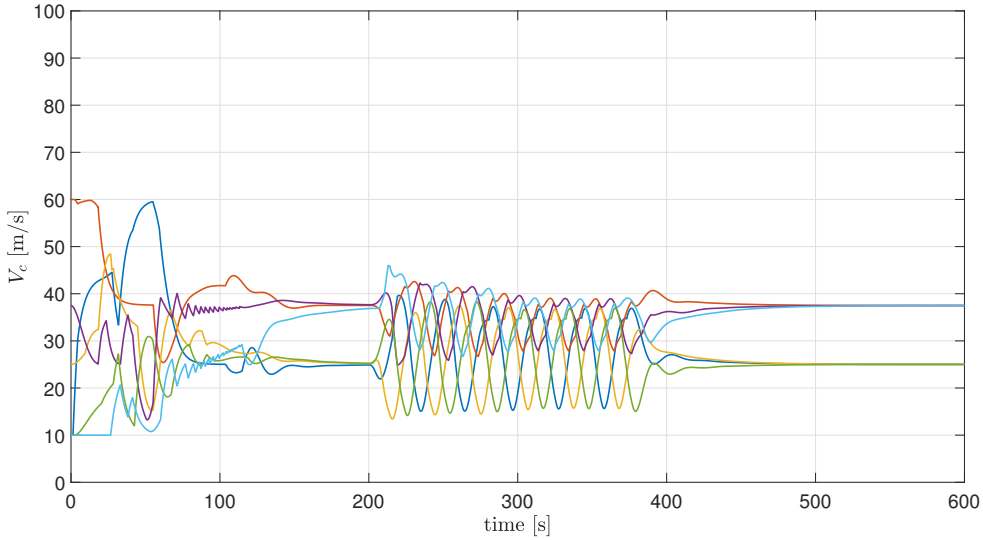


Figure 7. Actual speeds of the vehicles.

At $t = 200$ s, the target starts moving in the northeast direction at a speed of $V_t(t) = 5$ m/s. As it can be seen in Figure 7, the speeds of the vehicles oscillate around the desired values. The reason is that the trajectory of the UxVs at this time is not a circular orbit, as it is in the case of a stationary target (this can be noted from the trajectory of UxV1 depicted in Figure 3), and following this trajectory requires oscillatory (linear and angular) velocity commands. Finally, Figures 4–6 show the oscillatory behavior of the VBT and the coordination errors, which, however, remain bounded as expected.

At $t \approx 380$ s, the target reaches position $[200; 200]$ m and stops (i.e., $V_t(t) = 0$ m/s). Again, the speeds converge to the desired values, while the VBT and the coordination error converge close to zero.

A video of these results and the Matlab code used to generate the plots can be found at the following link: https://github.com/venanziocichella/Cooperative-Vision-Based-Tracking (accessed on 2 March 2023) .

5. Conclusions

In this paper, a solution for the coordinated vision-based tracking problem is given. The proposed control laws enable n unmanned vehicles (UxVs) to move around a target along n desired orbits, while coordinating with each other (i.e., maintaining a desired phase shift). The yaw rate is used to solve the vision-based tracking problem. The coordination between the UxVs is achieved by adjusting the speed of each vehicle. Non-perfect tracking performance of an on-board autopilot is considered. First, a solution to the vision-based tracking problem is given considering the case of a single UxV. Second, we provide a solution to the coordination problem. The simulation results validate the theoretical findings.

Author Contributions: Conceptualization, V.C. and I.K.; methodology, V.C. and I.K.; software, V.C and I.K.; validation, V.C and I.K.; investigation, V.C. and I.K.; resources, V.C. and I.K.; writing—original draft preparation, V.C. and I.K.; writing—review and editing, V.C and I.K.; supervision, V.C. and I.K.; project administration, V.C. and I.K.; funding acquisition, V.C. and I.K. All authors have read and agreed to the published version of the manuscript.

Funding: Venanzio Cichella was supported by Amazon and by the Office of Naval Research (grants N000141912106 and N000142112091). Isaac Kaminer was supported by the Office of Naval Research (grants N0001421WX01974, N0001419WX00155, N0001422WX01906) and NPS CRUSER.

Institutional Review Board Statement: Not applicable.

Informed Consent Statement: Not applicable.

Data Availability Statement: Not applicable.

Conflicts of Interest: The authors declare no conflict of interest.

Appendix A. Proof of Lemma 1

Consider System (3). Add and subtract $\dot{\psi}_c/\rho_d$ in the first equation, and substitute the control law in Equation (4) to obtain

$$\begin{cases} \dot{\hat{\eta}} = -\dfrac{V_g \cos(\hat{\eta}\rho_d)}{\rho_d}\rho_e - k_\eta \hat{\eta}(t) + \dfrac{\dot{\psi} - \dot{\psi}_c}{\rho_d} + \dfrac{V_t \cos(\hat{\eta}\rho_d - \psi_r)\left(\rho_e + \frac{1}{\rho_d}\right)}{\rho_d} \\ \dot{\rho}_e = \left(\rho_e + \dfrac{1}{\rho_d}\right)^2 V_g \sin(\eta) - \left(\rho_e + \dfrac{1}{\rho_d}\right)^2 V_t \sin(\hat{\eta}\rho_d - \psi_r)\,. \end{cases}$$

After simple algebraic manipulations, we can rewrite the previous system of equations as

$$\dot{x} = A_x x + f^*(x) + \begin{bmatrix} \frac{\dot{\psi} - \dot{\psi}_c}{\rho_d} \\ 0 \end{bmatrix},$$

where $x = [\hat{\eta}\,,\, \rho_e]^\top$,

$$A_x = \begin{bmatrix} -k_\eta & -V_g/\rho_d \\ V_g/\rho_d & 0 \end{bmatrix},$$

$$f^*(x) = \begin{bmatrix} V_g \rho_e (1 - \cos(\hat{\eta}\rho_d))/\rho_d \\ V_g(\rho_e + 1/\rho_d)^2 \sin(\hat{\eta}\rho_d) - \frac{V_g}{\rho_d}\hat{\eta} \end{bmatrix} + \begin{bmatrix} V_t(\rho_e + 1/\rho_d)\cos(\hat{\eta}\rho_d - \psi_r)/\rho_d \\ -V_t(\rho_e + 1/\rho_d)^2 \sin(\hat{\eta}\rho_d - \psi_r) \end{bmatrix}.$$

In [21], the authors show that $\forall x \in \Omega_v$, $f^*(x)$ satisfies the following bound

$$||f^*(x)|| \leq \frac{V_g}{\rho_d}\gamma||x|| + \frac{V_{t,max}(1 + c_\rho)}{\rho_d^2}\sqrt{1 + (1 + c_\rho)^2}, \tag{A1}$$

$$\gamma \triangleq c_\rho \sqrt{\frac{c_\rho^2}{4} + \left(2 + c_\rho + \frac{c_\rho}{6}\right)^2}.$$

Next, consider the following Lyapunov function

$$V(x) = x^\top P x\,, \quad P = \begin{bmatrix} \frac{\rho_d}{V_{g,min}} k_\eta & 1 \\ 1 & \frac{\rho_d}{V_{g,min}} k_\eta \end{bmatrix}. \tag{A2}$$

Letting

$$W = \begin{bmatrix} 2k_\eta^2 \frac{\rho_d}{V_{g,min}} - 2\frac{V_g}{\rho_d} & k_\eta \\ k_\eta & 2\frac{V_g}{\rho_d} \end{bmatrix} > 0\,,$$

and noting that $A_x^\top P + P A_x = -W$, the derivative of the Lyapunov function can be computed as

$$\dot{V} = -x^\top W x + 2 f^{*\top}(x) P x + 2 \begin{bmatrix} \frac{\dot{\psi} - \dot{\psi}_c}{\rho_d} \\ 0 \end{bmatrix}^\top P x\,.$$

Defining λ_v such that $0 < \lambda_v < \frac{\lambda_{min}(W)}{2\lambda_{max}(P)}$, and recalling Assumption 3 and the bound in Equation (A1), one can write

$$\begin{aligned} \dot{V} &\leq -\lambda_{min}(W)||x||^2 + 2\lambda_{max}(P)||f^*||||x|| + 2\frac{\delta_\psi}{\rho_d}\lambda_{max}(P)||x|| \\ &\leq -\left(\lambda_{min}(W) - 2\frac{\lambda_{max}(P)}{\rho_d} V_g \gamma\right)||x||^2 \\ &+ 2\frac{\lambda_{max}(P)}{\rho_d}\left(\frac{V_{t,max}(1+c_\rho)}{\rho_d}\sqrt{1+(1+c_\rho)^2} + \delta_\psi\right)||x|| \\ &\leq -2\lambda_v \lambda_{max}(P)||x||^2 \\ &+ 2\left(\frac{V_{t,max}(1+c_\rho)}{\rho_d^2}\sqrt{1+(1+c_\rho)^2} + \frac{\delta_\psi}{\rho_d}\right)\lambda_{max}(P)||x|| \\ &\leq -2\lambda_{max}(P)||x||\left(\lambda_v||x|| - \frac{V_{t,max}(1+c_\rho)\sqrt{1+(1+c_\rho)^2}}{\rho_d^2} - \frac{\delta_\psi}{\rho_d}\right). \end{aligned} \tag{A3}$$

It follows that $\dot{V} < 0$ if

$$\frac{V_{t,max}(1+c_\rho)\sqrt{1+(1+c_\rho)^2}}{\lambda_v \rho_d^2} + \frac{\delta_\psi}{\lambda_v \rho_d} < ||x||\,. \tag{A4}$$

Finally, we can conclude that if $V_{t,max}$ and δ_ψ are sufficiently small and satisfy Condition (14), then $||x|| \leq \frac{c_\rho}{\rho_d}$, $\forall t \geq 0$, which completes the proof.

Appendix B. Proof of Corollary 1

The proof follows easily from the proof of Lemma 1 given in Appendix A. Consider the candidate Lyapunov function introduced in Equation (A2). Letting $V_t = 0$ and $\delta_\psi = 0$, from Equation (A3) it follows that

$$\dot{V}(x(t)) \leq -2\lambda_v \lambda_{max}(P)||x(t)||^2 \leq -2\lambda_v V(x(t))\,.$$

Applying the comparison lemma, we obtain

$$||x(t)|| \leq \sqrt{\frac{\lambda_{max}(P)}{\lambda_{min}(P)}}||x(0)||e^{-\lambda_v t}\,.$$

Appendix C. Proof of Theorem 1

The proof of Theorem 1 unfolds in two main steps:

Part (a): Assuming that the speed of the UxVs $V_{g,i}\,, \forall i \in \{1\,, \ldots\,, n\}$ satisfies Assumption 1, and the Vision-Based Tracking error lies inside the bounded region Ω_v defined in Equation (11) at time $t = 0$, using the result obtained in Lemma 1, we demonstrate that the coordination error satisfies the bound given in Equation (15).
Part (b): We prove that if the initial conditions of the vision-based tracking error and coordination error satisfy $x(0) \in \Omega_v$ and $\zeta(0) \in \Omega_c$, respectively, then the control law for the speed $V_{c,i}$ given in Equation (8), together with the bounds presented in Assumption 3, satisfy Assumption 1 $\forall t \geq 0$; therefore, $x \in \Omega_v\,, \forall t \geq 0$.

Part (b) implies that Part (a) holds $\forall t \geq 0$, thus proving Theorem 1.

Appendix C.1. Part (a)

First, we note that the result given in Equation (13) follows directly from Lemma 1 if Assumption 1 is satisfied. Thus, we can state that

$$||x_i|| \leq \frac{c_\rho}{\rho_{d,max}}\,, \quad \forall i \in \{1, \ldots, n\}\,, \quad \forall t \geq 0\,.$$

Second, from [25] Lemma 5, it follows that if the matrix $\bar{L} = QLQ^\top$ satisfies Assumption 6; then, a generic system with dynamics

$$\dot{\phi} = -a\bar{L}\phi$$

converges exponentially to zero as follows:

$$||\phi(t)|| \leq k_\phi ||\phi(0)|| e^{-\bar{\gamma}t}\,,$$

with $k_\phi = 1\,, \bar{\gamma} \geq \frac{an\mu}{T(1+anT)^2}$. This implies that ([26] Theorem 4.12), for any constants m_3 and m_4 satisfying $0 < m_3 \leq m_4$, there exists a continuously differentiable, symmetric, positive definite matrix $M(t) \in \mathbb{R}^{n-1 \times n-1}$ that satisfies the following inequalities:

$$0 < m_1 I_{n-1} \triangleq \frac{m_3}{2an} I_{n-1} \leq M(t) \leq \frac{m_4}{2\bar{\gamma}} I_{n-1} \triangleq m_2 I_{n-1}\,, \tag{A5}$$

$$\dot{M} - a\bar{L}M - aM\bar{L} \leq -m_3 I_{n-1} \triangleq m_2 I_{n-1}\,. \tag{A6}$$

Now, let us consider the first derivative of λ_i, which can be rewritten as follows:

$$\dot{\lambda}_i = \frac{V_{c,i} \cos \eta_i}{\rho_i} - V_t \beta_i + \frac{(V_{g,i} - V_{c,i}) \cos \eta_i}{\rho_i}\,,$$

where $\beta_i = \cos(\psi_t - (\psi_i - \eta_i))/\rho_i$. Substituting the control law given by Equation (8), we obtain

$$\dot{\lambda}_i = u_{\text{coord},i} + u_{\text{coord},i} \rho_{d,i} \rho e, i - V_t \beta_i + \frac{(V_{g,i} - V_{c,i}) \cos \eta_i}{\rho_i}\,,$$

which can be written in vector form as

$$\dot{\lambda} = u_{\text{coord}} + \Delta_e u_{\text{coord}} - V_t \beta + \Delta_v\,,$$

with

$$\Delta_v = \begin{bmatrix} \frac{(V_{g,1} - V_{c,1}) \cos \eta_1}{\rho_1} \\ \vdots \\ \frac{(V_{g,n} - V_{c,n}) \cos \eta_n}{\rho_n} \end{bmatrix}\,,$$

$$\Delta_e = \begin{bmatrix} \rho_{d,1}\rho_{e,1} & 0 & \dots & 0 \\ 0 & \rho_{d,2}\rho_{e,2} & \dots & 0 \\ \vdots & \vdots & \ddots & \vdots \\ 0 & 0 & \dots & \rho_{d,n}\rho_{e,n} \end{bmatrix},$$

and λ , u_{coord}, and β being the set of the individual variables collected in a column vector (e.g., $\lambda = [\lambda_1, \dots, \lambda_n]^\top$).

Similarly, by defining $C^\top \triangleq [0_{n-1}\ I_{n-1}] \in \mathbb{R}^{n-1\times n}$ and $\frac{V_d}{\rho_d} \triangleq \frac{V_{d,1}}{\rho_{d,1}} = \dots = \frac{V_{d,n}}{\rho_{d,n}}$, Equation (9) can be written in vector form as

$$u_{coord} = -aL\lambda + \begin{bmatrix} \frac{V_d}{\rho_d} \\ \chi_I \end{bmatrix}, \quad \dot{\chi}_I = -bC^\top L\lambda\,,$$

Then, consider the coordination error vector $\zeta = [\zeta_1^\top\ , \zeta_2^\top]^\top$, where

$$\zeta_1 = Q\lambda\,, \quad \zeta_2 = \chi_I - \frac{V_d}{\rho_d}\,.$$

Differentiating ζ_1 with respect to time, we obtain

$$\begin{aligned} \dot{\zeta}_1 &= Q\dot{\lambda}\,, \\ &= Q(u_{\text{coord}} + \Delta_e u_{\text{coord}} - V_t\beta + \Delta_v)\,, \\ &= -a\bar{L}\zeta_1 + QC\zeta_2 - aQ\Delta_e LQ^\top\zeta_1 \\ &+ Q\Delta_e \begin{bmatrix} \frac{V_d}{\rho_d} \\ \vdots \end{bmatrix} + Q\Delta_e C\zeta_2 - QV_t\beta + Q\Delta_v\,. \end{aligned} \tag{A7}$$

Similarly, differentiating ζ_2, we have

$$\begin{aligned} \dot{\zeta}_2 &= \dot{\chi}_I\,, \\ &= -bC^\top L\lambda\,, \\ &= -bC^\top LQ^\top\zeta_1\,, \\ &= -bC^\top Q^\top\bar{L}\zeta_1\,. \end{aligned} \tag{A8}$$

Combining Equations (A7) and (A8), we can write the dynamics of the coordination error vector in compact form as follows:

$$\dot{\zeta} = A_\zeta\zeta + \bar{A}_\zeta\zeta + B_\zeta + B_{V_t} + B_{\Delta_v}\,,$$

where

$$A_\zeta = \begin{bmatrix} -a\bar{L} & QC \\ -bC^\top Q^\top\bar{L} & 0 \end{bmatrix},$$

$$\bar{A}_\zeta = \begin{bmatrix} -aQ\Delta_e LQ^\top & Q\Delta_e C \\ 0 & 0 \end{bmatrix},$$

$$B_\zeta = \begin{bmatrix} Q\Delta_e \begin{bmatrix} \frac{V_d}{\rho_d} \\ \vdots \end{bmatrix} \\ 0 \end{bmatrix}, \quad B_{V_t} = \begin{bmatrix} QV_t\beta \\ 0 \end{bmatrix}, \quad B_{\Delta_v} = \begin{bmatrix} Q\Delta_v \\ 0 \end{bmatrix}.$$

Let us apply the change of variables

$$z = S_\zeta\zeta\,, \quad S_\zeta = \begin{bmatrix} I_{n-1} & 0 \\ -\frac{b}{a}C^\top Q^\top & I_{n-1} \end{bmatrix}, \tag{A9}$$

with dynamics given by

$$\dot{z} = S_\zeta A_\zeta S_\zeta^{-1} z + S_\zeta \bar{A}_\zeta S_\zeta^{-1} z + S_\zeta (B_\zeta + B_{V_t} + B_{\Delta_v}) . \tag{A10}$$

Next, consider the following Lyapunov function candidate

$$V_c = z^\top M_c z , \tag{A11}$$

with

$$M_c = \begin{bmatrix} M & 0 \\ 0 & \frac{a^3}{b^3}(C^\top Q^\top Q C)^{-1} \end{bmatrix},$$

where M satisfies Equations (A5) and (A6). Noting that $\frac{1}{n} \leq \lambda(C^\top Q^\top Q C) \leq 1$, we can state that V_c is bounded as follows:

$$\min\left(m_1 , \frac{a^3}{b^3}\right)||z||^2 \leq V_c \leq \max\left(m_2 , \frac{a^3}{b^3} n\right)||z||^2 .$$

Computing the time derivative of V_c, and letting $Z = QC$, we obtain

$$\dot{V}_c = z^T \begin{bmatrix} \dot{M} - a\bar{L}M - aM\bar{L} \\ \quad + \frac{b}{a}(ZZ^TM + MZZ^T) & MZ - \frac{a}{b}Z \\ Z^TM - \frac{a}{b}Z^T & -2\frac{a^2}{b^2} I_{n-1} \end{bmatrix} z$$

$$+ z^T \begin{bmatrix} -aQL\Delta_e Q^T M - aMQ\Delta_e L Q^T & MQ\Delta_e C \\ + \frac{b}{a} Z C^T \Delta_e Q^T M & + \frac{a^3}{b^2} QL\Delta_e Q^T Z (Z^T Z)^{-1} \\ + \frac{b}{a} MQ\Delta_e C Z^T & - \frac{a}{b} Z C^T \Delta_e Q^T Z (Z^T Z)^{-1} \\ C^T \Delta_e Q^T M & \\ \quad + \frac{a^3}{b^2}(Z^TZ)^{-1} Z^T Q \Delta_e L Q^T & - \frac{a^2}{b^2}(C^T \Delta_e Q^T Z (Z^TZ)^{-1} \\ \quad - \frac{a}{b}(Z^TZ)^{-1} Z^T Q \Delta_e C Z^T & + (Z^TZ)^{-1} Z^T Q \Delta_e C) \end{bmatrix} z$$

$$+ (B_\zeta + B_{V_t} + B_{\Delta_v})^T S_\zeta M_c z + z^T M_c S_\zeta (B_\zeta + B_{V_t} + B_{\Delta_v}) .$$

Using Equation (A6), $||QC|| = ||Z|| = 1$, $||\Delta_e|| \leq \rho_{d,\max} \sup_{i \in \{1,\dots,n\}}(||x_i||) \leq c_\rho$ and $||L|| \leq n$, we can write

$$\begin{aligned} \dot{V}_c \leq\, & z^\top \begin{bmatrix} -m_3 I_{n-1} + \frac{b}{a}(ZZ^\top M + MZZ^\top) & (M - \frac{a}{b} I_{n-1}) Z \\ Z^\top (M - \frac{a}{b} I_{n-1}) & -2\frac{a^2}{b^2} I_{n-1} \end{bmatrix} z \\ & + z^\top \begin{bmatrix} \left(2am_2 n + 2\frac{b}{a} m_2 \right. & 0 \\ \left. + m_2 + \frac{a^3}{b^2} n^2 + \frac{a}{b} n\right) c_\rho & \\ 0 & \left(2\frac{a^2}{b^2} n + m_2 \right. \\ & \left. + \frac{a^3}{b^2} n^2 + \frac{a}{b} n\right) c_\rho \end{bmatrix} z \\ & + 2||B_\zeta + B_{V_t} + B_{\Delta_v}||||S_\zeta||||M_c||||z|| . \end{aligned} \tag{A12}$$

Letting

$$\lambda_M = \max\left(2am_2n + 2\frac{b}{a}m_2 + m_2 + \frac{a^3}{b^2}n^2 + \frac{a}{b}n\,,\, 2\frac{a^2}{b^2}n + m_2 + \frac{a^3}{b^2}n^2 + \frac{a}{b}n\right),$$

inequality Equation (A12) reduces to

$$\dot{V}_c \leq -z^\top W_c z + 2||B_\zeta + B_{V_t} + B_{\Delta_v}||||S_\zeta||||M_c||||z||\,,$$

with

$$W_c = \begin{bmatrix} (m_3 - \lambda_M c_\rho)I_{n-1} - \frac{b}{a}(ZZ^\top M + MZZ^\top) & \left(\frac{a}{b}I_{n-1} - M\right)Z \\ Z^\top\left(\frac{a}{b}I_{n-1} - M\right) & \left(2\frac{a^2}{b^2} - \lambda_M c_\rho\right)I_{n-1} \end{bmatrix}.$$

At this point, one can show (see Appendix E) that, for some choice of a, b, m_3, and m_4, the following inequality is satisfied:

$$W_c \geq 2\lambda_c V_c\,, \tag{A13}$$

where $\lambda_c = \frac{\bar{\gamma}}{(1+kn)\rho_k}$, which allows us to write

$$\dot{V}_c \leq -2\lambda_c V_c + 2\max\left(m_2\,,\,\frac{a^3}{b^3}n\right)\left(\frac{V_{d,max}}{\rho_{d,min}}\rho_{d,max}||x|| + \frac{V_{t,max}}{\rho_{min}} + \frac{\delta_V}{\rho_{min}}\right)||z||\,.$$

Applying [26] Theorem 4.19, and letting

$$u_{xv} = 3\max\left(\frac{V_{d,max}}{\rho_{d,min}}\rho_{d,max}||x||\,,\,\frac{V_{t,max}}{\rho_{min}}\,,\,\frac{\delta_V}{\rho_{min}}\right), \tag{A14}$$

one can conclude that the system Equation (A10) is ISS, with input $u_{xv}(t)$, and that the following inequality is satisfied $\forall t \geq 0$:

$$\begin{aligned} ||z(t)|| \leq & \sqrt{\frac{\max\left(m_2\,,\,\frac{a^3}{b^3}n\right)}{\min\left(m_1\,,\,\frac{a^3}{b^3}\right)}}||z(0)||e^{-\lambda_c(1-\theta)t} \\ & + \left(\frac{\max\left(m_2\,,\,\frac{a^3}{b^3}n\right)}{\min\left(m_1\,,\,\frac{a^3}{b^3}\right)}\right)^{\frac{3}{2}}\frac{1}{\lambda_c\theta}\left(\sup_{0\leq\tau\leq t}||u_{xv}(\tau)||\right), \end{aligned}$$

with θ satisfying $0 < \theta < 1$. Finally, recalling the transformation given in Equation (A9), we can conclude that

$$||\zeta(t)|| \leq \kappa_1||\zeta(0)||e^{-\lambda_c(1-\theta)t} + \kappa_2\left(\sup_{0\leq\tau\leq t}||u_{xv}(\tau)||\right), \tag{A15}$$

with

$$\begin{aligned} \kappa_1 &= ||S_\zeta^{-1}||\sqrt{\frac{\max\left(m_2\,,\,\frac{a^3}{b^3}n\right)}{\min\left(m_1\,,\,\frac{a^3}{b^3}\right)}}||S_\zeta||\,, \\ \kappa_2 &= ||S_\zeta^{-1}||\left(\frac{\max\left(m_2\,,\,\frac{a^3}{b^3}n\right)}{\min\left(m_1\,,\,\frac{a^3}{b^3}\right)}\right)^{\frac{3}{2}}\frac{1}{\lambda_c\theta}\,. \end{aligned} \tag{A16}$$

Appendix C.2. Part (b)

We will prove the claim by contradiction. Assume that at some time $t > 0$ the Vision-Based Tracking error of the i-th UxV is such that $x_i(t) \notin \Omega_v$. Thus, there exists a time t' such that

$$V(x_i(t')) = c_v^2, \quad \dot{V}(x_i(t')) > 0, \tag{A17}$$

while

$$V(x_i(\tau)) \leq c_v^2, \forall \tau \in [0, t'). \tag{A18}$$

Notice that Equations (A17) and (A18) imply that

$$\rho_{e,i}(\tau) \leq \frac{c_\rho}{\rho_{d,max}}, \quad \eta_i(\tau) \leq c_\rho, \quad \forall \tau \in [0, t'],$$

where

$$c_\rho < \min\left(\frac{1}{2kn((1+a)n+1+a)\rho_k^2}, \frac{V_{g,max} - V_{d,max}/c_\eta}{2\kappa_2(an+1)}, \frac{V_{d,min} - V_{g,min}}{2\kappa_2(an+1)} \right).$$

The choice of k and ρ_k in Appendix E, together with the definition of c_ρ, implies that there exists a positive constant c_η such that $\cos(\eta_i(\tau)) \geq cos(c_\rho) \geq c_\eta > \frac{1}{2}$; therefore, the velocity command $V_{g,i}(\tau)$ given in (8) is well-defined $\forall \tau \in [0, t']$. Moreover, from the proof given in Appendix C, Part (a), it follows that the coordination error at time t' satisfies

$$||\zeta(t')|| \leq \kappa_1 ||\zeta(0)|| e^{-\lambda_c(1-\theta)t'} + \kappa_2 \left(\sup_{0 \leq \tau \leq t'} ||u_{xv}(\tau)|| \right), \tag{A19}$$

where, by assumption, $||\zeta(0)|| \leq c_c$ with

$$c_c \triangleq \min\left(\frac{V_{g,max} - V_{d,max}/c_\eta}{2\kappa_1 \rho_{d,max}(an+1)} - \frac{\kappa_2}{\kappa_1}\frac{c_\rho}{\rho_{d,max}}, \frac{V_{d,min} - V_{g,min}}{2\kappa_1 \rho_{d,max}(an+1)} - \frac{\kappa_2}{\kappa_1}\frac{c_\rho}{\rho_{d,max}} \right),$$

Consider now the speed of the i-th vehicle at time τ given by

$$V_{g,i}(t') = \frac{u_{coord,i}(t')\rho_{d,i}}{cos(\eta_i(t'))}.$$

Noting that $u_{coord,i}$ satisfies

$$-(an+1)||\zeta(t')|| + \frac{V_{d,i}}{\rho_{d,i}} \leq u_{coord,i}(t') \leq (an+1)||\zeta(t')|| + \frac{V_{d,i}}{\rho_{d,i}},$$

we can find the following bound for the speed

$$-2(an+1)\rho_{d,i}||\zeta(t')|| + V_{d,i} \leq V_{g,i}(t') \leq 2(an+1)\rho_{d,i}||\zeta(t')|| + \frac{V_{d,i}}{c_\eta}.$$

Hence, from the result in Equation (A19), from the choice of c_v and c_c, and for sufficiently small values of $V_{t,max}$, the following bound is verified at time t':

$$V_{g,min} \leq V_{g,i}(t') \leq V_{g,max}.$$

Using the proof given in Appendix A, we can show that $\dot{V}(x(t')) < 0$, thus contradicting the claim in Equation (A17).

Appendix D. Proof of Corollary 2

Since $V_t = \delta_V = \delta_\psi = 0$, from Corollary 1, we obtain the following result

$$||x(t)|| \leq \sqrt{\frac{\lambda_{max}(P)}{\lambda_{min}(P)}}||x(0)||e^{-\lambda_v t}. \tag{A20}$$

Now, rewrite inequality Equation (A15) as follows:

$$||\zeta(t)|| \leq \kappa_1||\zeta(s)||e^{-\lambda_c(1-\theta)(t-s)} + \kappa_2\left(\sup_{s\leq\tau\leq t}||u_{xv}(\tau)||\right), \tag{A21}$$

where $t \geq s \geq 0$. Apply Equation (A21) with $s = t/2$ to obtain

$$||\zeta(t)|| \leq \kappa_1||\zeta(t/2)||e^{-\lambda_c(1-\theta)(t/2)} + \kappa_2\left(\sup_{t/2\leq\tau\leq t}||u_{xv}(\tau)||\right). \tag{A22}$$

Apply Equation (A21) with $s = 0$ and t replaced by $t/2$ to obtain the estimate of $\zeta(t/2)$ as

$$||\zeta(t/2)|| \leq \kappa_1||\zeta(0)||e^{-\lambda_c(1-\theta)(t/2)} + \kappa_2\left(\sup_{0\leq\tau\leq t/2}||u_{xv}(\tau)||\right). \tag{A23}$$

Combining Equations (A22) and (A23), we obtain

$$\begin{aligned}||\zeta(t)|| \leq \kappa_1 e^{-\lambda_c(1-\theta)(t/2)}\Big(\kappa_1||\zeta(0)||e^{-\lambda_c(1-\theta)(t/2)} + \\ \kappa_2\sup_{0\leq\tau\leq t/2}||u_{xv}(\tau)||\Big) + \kappa_2\sup_{t/2\leq\tau\leq t}||u_{xv}(\tau)||.\end{aligned} \tag{A24}$$

Notice that from $V_t = \delta_V = 0$ it follows that

$$\sup_{0\leq\tau\leq t}||u_{xv}(\tau)|| = \frac{V_{d,max}\rho_{d,max}}{\rho_{d,min}}\sup_{0\leq\tau\leq t}||x(\tau)||.$$

Using Equation (A20), we can write

$$\begin{aligned}\sup_{0\leq\tau\leq t/2}(||x(\tau)||) &\leq \sqrt{\frac{\lambda_{max}(P)}{\lambda_{min}(P)}}||x(0)||, \\ \sup_{t/2\leq\tau\leq t}(||x(\tau)||) &\leq \sqrt{\frac{\lambda_{max}(P)}{\lambda_{min}(P)}}||x(0)||e^{-\lambda_v t/2}\end{aligned}$$

Therefore, combining Equation (A24) with the previous two inequalities, and letting

$$\bar{\kappa}_1 \triangleq \kappa_1^2, \quad \bar{\kappa}_2 \triangleq (1+\kappa_1)\kappa_2\sqrt{\frac{\lambda_{max}(P)}{\lambda_{min}(P)}}\frac{V_{d,max}\rho_{d,max}}{\rho_{d,min}}, \tag{A25}$$

we obtain

$$||\zeta(t)|| \leq \bar{\kappa}_1||\zeta(0)||e^{-\lambda_c t} + \bar{\kappa}_2||x(0)||e^{-\frac{\lambda_v+\lambda_c}{2}t},$$

thus proving Corollary 2.

Appendix E. Proof of Inequality Equation (A13)

To prove inequality Equation (A13), we need to show that the following matrix is positive semi-definite:

$$\begin{bmatrix} (m_3 - 2\lambda_c m_2) I_{n-1} & \\ -\frac{b}{a}(ZZ^\top M + MZZ^\top) & (\frac{a}{b} I_{n-1} - M) Z \\ -\lambda_M c_\rho I_{n-1} & \\ Z^\top (\frac{a}{b} I_{n-1} - M) & 2\frac{a^2}{b^2}\left(I_{n-1} - \frac{a}{b}\lambda_c n I_{n-1}\right) \\ & -\lambda_M c_\rho I_{n-1} \end{bmatrix} \geq 0\,. \tag{A26}$$

Using the Shur complement, sufficient conditions for Equation (A26) to hold are

$$2\frac{a^2}{b^2}\left(I_{n-1} - \frac{a}{b}\lambda_c n I_{n-1}\right) - \lambda_M c_\rho I_{n-1} > 0\,, \tag{A27}$$

and

$$\begin{aligned} &(m_3 - 2\lambda_c m_2) I_{n-1} - \frac{b}{a}(ZZ^\top M + MZZ^\top) - \lambda_M c_\rho I_{n-1} \\ &- \left(\frac{a}{b} I_{n-1} - M\right) Z \left(2\frac{a^2}{b^2}(I_{n-1} - \frac{a}{b}\lambda_c n I_{n-1}) - \lambda_M c_\rho I_{n-1}\right)^{-1} Z^\top \left(\frac{a}{b} I_{n-1} - M\right) \geq 0 \end{aligned} \tag{A28}$$

Equation (A27) is satisfied if the following holds:

$$2\frac{a^2}{b^2}\left(1 - \frac{a}{b}\lambda_c n - \frac{b^2}{a^2}\lambda_M c_\rho\right) > 0\,.$$

Letting $\lambda_c = \frac{\bar{\gamma}}{(1+kn)\rho_k}$ and $\frac{a}{b} = \frac{(kn+1)\rho_k}{\bar{\gamma} kn}$, the previous inequality reduces to

$$2\frac{a^2}{b^2}\left(1 - \frac{1}{k} - \frac{b^2}{a^2}\lambda_M c_\rho\right) > 0\,. \tag{A29}$$

Now, consider the term $\frac{b^2}{a^2}\lambda_M c_\rho$ and recall that

$$\lambda_M = \max\left(2am_2 n + 2\frac{b}{a}m_2 + m_2 + \frac{a^3}{b^2}n^2 + \frac{a}{b}n\,,\, 2\frac{a^2}{b^2}n + m_2 + \frac{a^3}{b^2}n^2 + \frac{a}{b}n\right),$$

Letting $m_3 = m_4 = \frac{2\rho_k(1+kn)}{kn}$, noting that $m_2 = \frac{m_4}{2\bar{\gamma}} = \frac{a}{b}$, choosing $\rho_k > 1$, and recalling the fact that $c_\rho < \frac{1}{2kn((1+a)n+1+a)\rho_k^2}$, one can show that the following relation holds:

$$\frac{b^2}{a^2}\lambda_M c_\rho \leq \frac{1}{k\rho_k^2}\,,$$

Therefore, Equation (A29) is satisfied if the following inequality is true:

$$2\frac{a^2}{b^2}\left(1 - \frac{2}{k}\right) > 0\,,$$

which is guaranteed from the choice $k > 2$.

Now, consider inequality Equation (A28). Defining

$$\alpha \triangleq \left(I_{n-1} - \frac{a}{b}\lambda_c n I_{n-1} - \frac{b^2}{a^2}\lambda_M c_\rho I_{n-1}\right)^{-1},$$

we obtain

$$(m_3 - 2\lambda_c m_2) I_{n-1} - \frac{b}{a}(ZZ^\top M + MZZ^\top) - \lambda_M c_\rho I_{n-1} - \left(\frac{a}{b} I_{n-1} - M\right) Z \left(\frac{b^2}{2a^2}\alpha^{-1}\right) Z^\top \left(\frac{a}{b} I_{n-1} - M\right) \geq 0\,.$$

Using the fact that $||Z|| = 1$, $||M|| \leq \frac{m_3}{2\bar{\gamma}}$, and after straightforward computations, the previous inequality reduces to

$$m_3\left(1 - \frac{\lambda_c}{\bar{\gamma}}\right) - 2\left(1 - \frac{\alpha}{2}\right) - \frac{a^2}{b^2}\frac{1}{kn\rho_k^2} - \frac{1}{2}\alpha - \frac{1}{8}\frac{b^2}{a^2} m_3^2 \geq 0\,. \tag{A30}$$

Finally, substituting

$$m_3 = \frac{2\rho_k(1+kn)}{kn}\,, \quad \lambda_c = \frac{\bar{\gamma}}{(1+kn)\rho_k}\,, \quad \frac{a}{b} = \frac{(1+kn)\rho_k}{\bar{\gamma}kn}\,,$$

and choosing

$$\rho_k \geq \max\left(\frac{2k\bar{\gamma}}{1+kn}\,, 1\,, \left(1 + \frac{1}{4}\bar{\gamma}^2 + \frac{(kn+1)^2}{\bar{\gamma}^2 k^2 n^3}\right)\right), \tag{A31}$$

we can show that Equation (A30) is verified, which completes the proof.

References

1. Mcfadyen, A.; Mejias, L. A survey of autonomous vision-based see and avoid for unmanned aircraft systems. *Prog. Aerosp. Sci.* **2016**, *80*, 1–17. [CrossRef]
2. Al-Kaff, A.; Armingol, J.M.; de La Escalera, A. A vision-based navigation system for Unmanned Aerial Vehicles (UAVs). *Integr. Comput. Aided Eng.* **2019**, *26*, 297–310. [CrossRef]
3. Asl, H.J. Robust vision-based tracking control of VTOL unmanned aerial vehicles. *Automatica* **2019**, *107*, 425–432.
4. Cichella, V.; Kaminer, I.; Dobrokhodov, V.; Hovakimyan, N. Coordinated vision-based tracking for multiple UAVs. In Proceedings of the 2015 IEEE/RSJ International Conference on Intelligent Robots and Systems (IROS), Hamburg, Germany, 28 September–2 October 2015; IEEE: New York, NY, USA, 2015; pp. 656–661.
5. Lawrence, A. *Modern Inertial Technology: Navigation, Guidance, and Control*; Springer: Berlin/Heidelberg, Germany, 1998.
6. Redding, J.D.; McLain, T.W.; Beard, R.W.; Taylor, C.N. Vision-based target localization from a fixed-wing miniature air vehicle. In Proceedings of the American Control Conference, Minneapolis, MN, USA, 14–16 June 2006; IEEE: New York, NY, USA, 2006; p. 6.
7. Campbell, M.E.; Wheeler, M. Vision-based geolocation tracking system for uninhabited aerial vehicles. *J. Guid. Control. Dyn.* **2010**, *33*, 521–532. [CrossRef]
8. Bar-Shalom, Y. *Tracking and Data Association*; Academic Press Professional, Inc.: Cambridge, MA, USA, 1987.
9. Ljung, L. Asymptotic behavior of the extended Kalman filter as a parameter estimator for linear systems. *Autom. Control. IEEE Trans.* **1979**, *24*, 36–50. [CrossRef]
10. Ghyzel, P.A. Vision-Based Navigation for Autonomous Landing of Unmanned Aerial Vehicles. Ph.D. Thesis, Naval Postgraduate School, Monterey, CA, USA, 2000.
11. Valasek, J.; Gunnam, K.; Kimmett, J.; Junkins, J.L.; Hughes, D.; Tandale, M.D. Vision-based sensor and navigation system for autonomous air refueling. *J. Guid. Control. Dyn.* **2005**, *28*, 979–989. [CrossRef]
12. Aicardi, M.; Casalino, G.; Bicchi, A.; Balestrino, A. Closed loop steering of unicycle like vehicles via Lyapunov techniques. *Robot. Autom. Mag. IEEE* **1995**, *2*, 27–35. [CrossRef]
13. Frew, E.W.; Lawrence, D.A.; Morris, S. Coordinated standoff tracking of moving targets using Lyapunov guidance vector fields. *J. Guid. Control. Dyn.* **2008**, *31*, 290–306. [CrossRef]
14. Kaminer, I.; Pascoal, A.M.; Xargay, E.; Hovakimyan, N.; Cichella, V.; Dobrokhodov, V. *Time-Critical Cooperative Control of Autonomous Air Vehicles*; Butterworth-Heinemann: Oxford, UK, 2017.
15. Cichella, V.; Choe, R.; Mehdi, S.B.; Xargay, E.; Hovakimyan, N.; Dobrokhodov, V.; Kaminer, I.; Pascoal, A.M.; Aguiar, A.P. Safe coordinated maneuvering of teams of multirotor unmanned aerial vehicles: A cooperative control framework for multivehicle, time-critical missions. *IEEE Control Syst. Mag.* **2016**, *36*, 59–82.
16. Mesbahi, M.; Hadaegh, F.Y. Formation flying control of multiple spacecraft via graphs, matrix inequalities, and switching. *J. Guid. Control. Dyn.* **2001**, *24*, 369–377. [CrossRef]
17. Pereira, F.L.; De Sousa, J.B. Coordinated control of networked vehicles: An autonomous underwater system. *Autom. Remote Control* **2004**, *65*, 1037–1045. [CrossRef]

18. Stipanović, D.M.; Inalhan, G.; Teo, R.; Tomlin, C.J. Decentralized overlapping control of a formation of unmanned aerial vehicles. *Automatica* **2004**, *40*, 1285–1296. [CrossRef]
19. Ma, L.; Hovakimyan, N. Vision-based cyclic pursuit for cooperative target tracking. *J. Guid. Control. Dyn.* **2013**, *36*, 617–622. [CrossRef]
20. Ma, L.; Hovakimyan, N. Cooperative target tracking with time-varying formation radius. In Proceedings of the European Control Conference, Linz, Austria, 15–17 July 2015; IEEE: New York, NY, USA, 2015.
21. Dobrokhodov, V.; Kaminer, I.; Jones, K.; Ghabcheloo, R. Vision-based tracking and motion estimation for moving targets using unmanned air vehicles. *J. Guid. Control. Dyn.* **2008**, *31*, 907–917. [CrossRef]
22. Cichella, V.; Kaminer, I.; Dobrokhodov, V.; Hovakimyan, N. Cooperative Vision-Based Tracking of Multiple UAVs. In Proceedings of the AIAA Guidance, Navigation, and Control Conference, Boston, MA, USA, 19–22 August 2013.
23. Xargay, E.; Kaminer, I.; Pascoal, A.; Hovakimyan, N.; Dobrokhodov, V.; Cichella, V.; Aguiar, A.P.; Ghabcheloo, R. Time-Critical Cooperative Path Following of Multiple Unmanned Aerial Vehicles over Time-Varying Networks. *AIAA J. Guid. Control. Dyn.* **2013**, *36*, 499–516. [CrossRef]
24. Biggs, N. *Algebraic Graph Theory*; Cambridge University Press: New York, NY, USA, 1993.
25. Panteley, E.; Loría, A. Uniform Exponential Stability for Families of linear Time-Varying Systems. In Proceedings of the IEEE Conference on Decision and Control, Sydney, Australia, 12–15 Decemebr 2000; pp. 1948–1953.
26. Khalil, H.K. *Nonlinear Systems*; Prentice Hall: Englewood Cliffs, NJ, USA, 2002.

Disclaimer/Publisher's Note: The statements, opinions and data contained in all publications are solely those of the individual author(s) and contributor(s) and not of MDPI and/or the editor(s). MDPI and/or the editor(s) disclaim responsibility for any injury to people or property resulting from any ideas, methods, instructions or products referred to in the content.